Front. Earth Sci. 2017, 11(3): 515–530
DOI 10.1007/s11707-016-0630-z

RESEARCH ARTICLE

Effect of snow on mountain river regimes: an example from the Pyrenees

Alba SANMIGUEL-VALLELADO (✉)[1], Enrique MORÁN-TEJEDA[1,2], Esteban ALONSO-GONZÁLEZ[1], Juan Ignacio LÓPEZ-MORENO[1]

1 Pyrenean Institute of Ecology, CSIC (Spanish Research Council), Zaragoza, Spain
2 Department of Geography, University of the Balearic Islands, Palma de Mallorca, Spain

Abstract The purpose of this study was to characterize mountain river regimes in the Spanish Pyrenees and to assess the importance of snow accumulation and snowmelt on the timing of river flows. Daily streamflow data from 9 gauging stations in the Pyrenees were used to characterize river regimes. These data were analyzed by hydrological indices, with a focus on periods when snow accumulation and snowmelt occurred. These results were combined with data on Snow Water Equivalent (SWE) (from measurements of depth and density of snow in the main river basins and also simulated by a process-based hydrological model), snowmelting (simulated by a process-based hydrological model), precipitation (from observations), and temperature (from observations). Longitude and elevation gradients in the Pyrenees explain the transition of river regimes from those that mostly had low nival signals (in the west and at low elevations) to those that mostly had high nival signals (low winter runoff and late spring peakflow, in the east and at high elevations). Although trend analyses indicated no statistically significant changes, there was a trend of decreased nival signal over time in most of the analyzed rivers. Our results also demonstrated that snow processes cannot explain all of the interannual variability of river regimes, because the temporal distribution of liquid precipitation and temperature play key roles in hydrography.

Keywords river regime, precipitation, snow indices, Spanish Pyrenees, streamflow

1 Introduction

Mountains are significant sources of freshwater worldwide and their role as water reservoirs is especially significant in arid and semi-arid regions (Viviroli et al., 2007; Masiokas et al., 2010; Chauvin et al., 2011; Foy et al., 2015). Such is the case in the Mediterranean region, where water balance (precipitation minus evapotranspiration) in the lowlands is generally negative, and hydrological hazards (floods and droughts) occur periodically (García-Ruiz et al., 2011). Thus, mountain systems such as the Pyrenees are the major source of most freshwater for populations that live downstream. The Ebro basin, located in northeast Spain, is a clear example of an area with strong pressure on water resources, due to the scarce precipitation, high rate of evapotranspiration (López-Moreno et al., 2011a), and water demand for agriculture, industry, and domestic uses. In this basin, the Pyrenees generate nearly half of the annual runoff (López and Justribó, 2010).

Snow dynamics play an important hydrological role in mountain systems that supply freshwater. Water reserves and seasonal variability of streamflow are both related to the timing of snow accumulation and snowmelt (López-Moreno and García-Ruiz, 2004; Stewart, 2009). Thus, the mountains serve as a natural reservoir during winter, when they accumulate solid precipitation (Stewart, 2009), and this snow ultimately provides water to most Pyrenean rivers. High flows occur during spring and early summer, when snowmelt contributes more to runoff than rainfall in most of the Pyrenean basins (López-Moreno and García-Ruiz, 2004). The presence of these events in an annual hydrograph indicates the presence of a nival river regime.

Snow-dominated basins are especially sensitive to climate variations (Barnett et al., 2005), and many recent studies have aimed to quantify the effects of past changes and predict future changes of snowpack in the context of the climate warming (López-Moreno, 2005; López-Moreno et al., 2009; Stewart, 2009; Beniston, 2012; Dedieu et al., 2014; Lute et al., 2015; Sankey et al., 2015) and seasonal patterns of streamflow (López-Moreno et al., 2014; Morán-Tejeda et al., 2014; Schnorbus et al., 2014).

Received July 8, 2016; accepted November 17, 2016

E-mail: albasv@ipe.csic.es

The main impacts of global warming on snow hydrology are: (a) reduced solid precipitation and a fractional increase of liquid precipitation during winter, and (b) an earlier snowmelt, leading to shorter snowpack duration. Taken together, these changes produce greater winter runoff, and lower spring and summer flows (Adam et al., 2009). However, not all local responses are consistent with these general findings (Stewart, 2009). All of these changes may increase as the climate continues to warm and this could exacerbate problems associated with management of water resources (Whitaker et al., 2008).

The main water management problems in the Ebro Basin occur because the supply of large volumes of water to the irrigated areas in the lowlands depend very much on snowmelt and its contribution to reservoirs (López-Moreno and García-Ruiz, 2004; López-Moreno, 2005). In fact, there have already been significant adjustments to water outflows from the main Pyrenean reservoirs to meet the increasing water demand due to decreasing runoff from the headwaters (López-Moreno et al., 2008, 2014). These changes are very likely to also affect aquatic ecosystems and other ecosystems, and have detrimental effects on ecosystem productivity and species composition (Auble et al., 1994; Hinch et al., 1995; Poff et al., 2002). To ensure the sustainable management of these natural resources and to better anticipate the impacts of climate warming, it is important to characterize the influence of the snowpack on streamflow timing and to identify future trends (Whitaker et al., 2008).

The first objective of this paper was to establish a typology of nival river regimes in different Pyrenean rivers for the period of 1950 to 2010, based on classification by several hydrological indices. The second objective was to determine the spatial and temporal variability of the different types of nival regimes. The last objective was to assess the importance of snow accumulation and melt on the nival character of these rivers, and thus the shape of their hydrographs, by comparison with other variables (precipitation and temperature).

2 Study area

The studied rivers are located in the NE of the Iberian Peninsula, and are some of the most important Pyrenean tributaries of the Ebro River (Fig. 1). The river network strongly splits up the relief due to the dominant North–South disposition of the main valleys, which are perpendicular to the West–East aligned Pyrenean structures (Peña and Lozano, 2004). The Pyrenean headwaters only account for 12% of the Ebro basin surface, but produce 56% of its total runoff (López-Moreno et al., 2011a). The elevation of the basin ranges from 450 to more than 3000 m a.s.l., and increases from west to east and from south to north. The annual 0°C isotherm is close to 2900 m a.s.l. (Marti et al., 2015; López-Moreno et al., 2016). The mean temperature is generally below 0°C from December to April above 1600 m a.s.l., and this is the

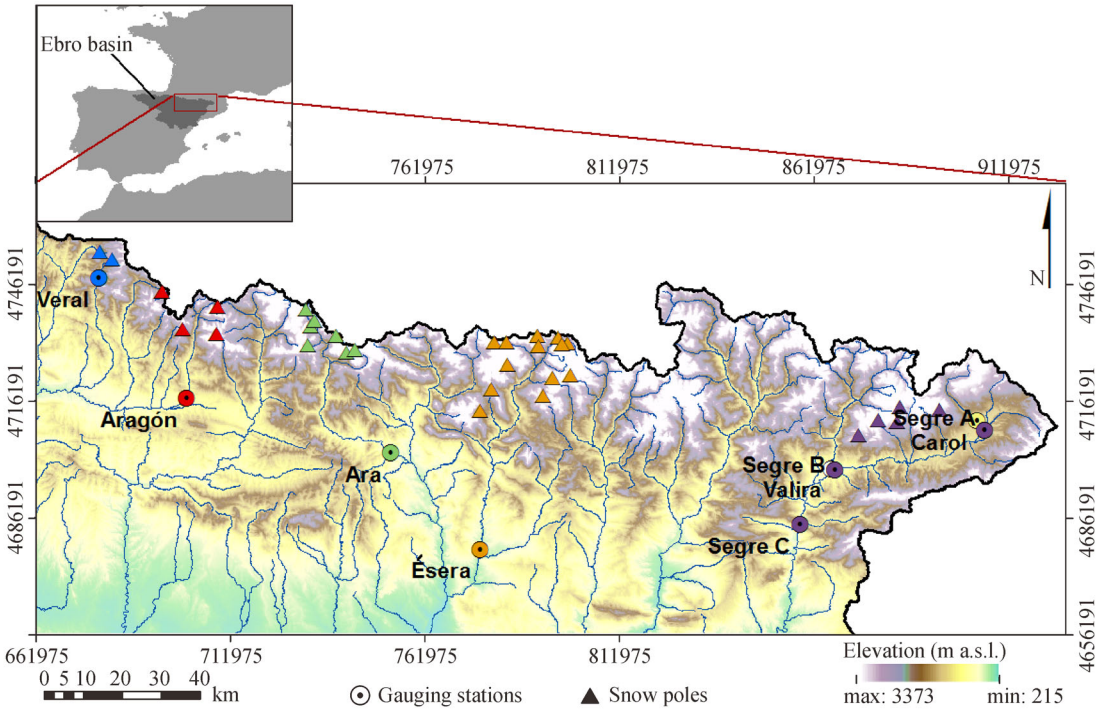

Fig. 1 Map of the Iberian Peninsula and the study area. Gauging stations: circles. Snow poles: triangles.

approximate limit for the seasonal snowpack (López-Moreno et al., 2011a). The relief is responsible for the precipitation gradient from the Ebro depression; annual mean values are below 400 mm at the middle of the depression and more than 2000 mm at the summits of the Pyrenees (García-Ruiz et al., 1985; López-Moreno and García-Ruiz, 2004; López and Justribó, 2010). There are some climatic variations between the western part of the study area (where the Atlantic Ocean has a strong influence) and the eastern part (where the more continental and Mediterranean climate has a strong influence) (Del Barrio et al., 1990).

3 Methods

3.1 Streamflow, snow and climate data

Daily streamflow data were collected from the Ebro Basin Authorities (C.H.E.) and downloaded from *Centro de Estudios Hidrográficos* (CEDEX, http://hercules.cedex.es/anuarioaforos/default.asp). We initially examined data from 44 gauging stations in the study area, and then selected the records of stations with the following criteria:

- At least 25 consecutive hydrological years (from October 1 to September 30), with a maximum of 5% of data gaps, until the last recorded and published year (2010).
- Location in the Pyrenean headwaters, and hence with an expected nival signal in the river regime. For this criterion, we performed visual inspections of the hydrographs, and checked that at least 50% of the annual streamflow recorded at each station was between March and July, the period suitable for detecting snowmelt in the selected Pyrenean mountain river regimes in view of the periods used by previous studies (López-Moreno and García-Ruiz, 2004; Clow, 2010).
- Absence of any hydraulic infrastructure upstream of the gauging station to ensure that natural streamflow timing was studied.

Nine of the 44 daily streamflow series met these criteria and all had records from 1985 to 2010. We also analyzed available longer data series that had up to 61 recorded years. Selected gauging stations were located in the Veral, Aragón, Ara, Ésera, Segre (with three of them), Valira, and Carol Rivers (Table 1). We estimated missing data using fitted linear models between the candidate series (series with missing data) and the reference series (the best correlated neighbor series: $R > 0.7$).

Snowpack data was collected from 31 snow poles that were in the headwaters of the main studied basins (Ara, Aragón, Ésera, Segre, and Veral) since 1986. These snow poles are part of a national network that measures snow depth, and are managed by the ERHIN Programme (Evaluación de los Recursos Hídricos procedentes de la INnivación) and dependent on the Ministry of the Environment. During each measurement period (January, March, and end of April), the snow depth is measured at each snow pole; snow density is recorded at some of the poles. The location of the snow poles aimed the representativeness of large areas, avoiding possible local anomalies caused by wind or snow avalanches. Despite this data suffer of limited temporal resolution and it does not reflect small scales snow variability of the snowpack (López-Moreno et al., 2011b), it has proven that they represent a useful information to characterize regional anomalies of snow accumulation and their relation with climatic and hydrological fluctuations (López-Moreno and García-Ruiz, 2004; López-Moreno, 2005; Morán-Tejeda et al., 2013). Only two snow poles had complete snow depth registers (1986–2010 hydrological years); all other selected snow poles had less than 35% missing data. The same method as described above was used for extrapolation of missing data in the snow depth series. Ultimately, 22, 25, and 20 complete series were obtained for January, March, and April, respectively. Snow Water Equivalent (SWE) series were calculated as the product of snow density and depth for each snow pole. We used the mean density value of each measurement period (Revuelto-Benedí et al., 2012), given that snow density values were not available for all poles. The coefficient of variation for snow density was lower than that for snow depth (López-Moreno et al., 2013).

In addition, we used two daily mean SWE and snowmelt

Table 1 Studied rivers and geographic characteristics

River name	Station location	Station basin surface/km^2	River basin surface > 2000 m a.s.l./%	Station height /m	Maximum height of basin/m	Series
Ara	Boltaña (Huesca)	626	18	680	3355	1951–2010
Aragón	Jaca (Huesca)	238	22	793	2886	1950–2010
Carol	Puigcerdá (Girona)	145	66	1189	2921	1985–2010
Ésera	Graus (Huesca)	893	27	450	3404	1950–2010
Segre (A, B, C)	Puigcerdá (Girona), La Seu D'Urgell (Lleida), Orgaña (Lleida)	297, 1233, 2384	33, 28, 27	1120, 670, 542,	2921	(1950, 1985, 1950) – 2010
Valira	La Seu D'Urgell (Lleida)	559	48	697	2865	1985–2010
Veral	Zuriza (Huesca)	47	14	1187	2366	1975–2010

series for the Aragón and Ésera river basins for 1979–2005. These series were from simulations performed with the Soil and Water Assessment Tool (SWAT), a hydrological model described by Morán-Tejeda et al. (2015). These data were used as a second source of snow data and for comparison with the results from ERHIN data in two of the most representative studied basins.

Finally, we obtained daily precipitation and maximum/minimum daily temperature series for the Aragón and Ésera river basins from the gridded Spain02 dataset (Herrera et al., 2012).

3.2 Statistical analysis

3.2.1 Identification of the types of river regimes

The original daily streamflow series were standardized for all years by dividing the daily data by the average streamflow for the period of December 1 to July 31. We selected the average of this period for standardization according to López-Moreno and García-Ruiz (2004), because this is the main period of snow accumulation and snowmelt. This standardization procedure allowed comparison of all gauging stations and all hydrological years, regardless of total river flows. It also allows a more precise determination of the timing of the main hydrological events related to snow accumulation and snowmelt. Each series was smoothed with a 30-day running mean to reduce the effect of isolated extreme events: the first element of the smoothed series was obtained by taking the average of the first 30 numbers of the original series; then the subset was modified excluding the first element of the original series and including the 30 + 1 number, this new subset was averaged again obtaining the second element of the smoothed series. This process was repeated to the end of the series.

River regimes were characterized based on the December–July hydrographs (Fig. 2). For this, we calculated several hydrological indices for each year for the discharge series of each of the 9 gauging stations by adapting to our analyzed period using various approaches specified in Table 2. Two types of indices can be distinguished: one type shows the relationship between the discharge value at a given time or period and the December–July average discharge (maxs, mins, maxw, minw, MAMJJ, p5, p95); the other type identifies the Julian day when a certain event is observed (dmaxs, dmins, dmaxw, dminw, do, de, d10, d30, d50, d70, d90).

We used a methodology to classify the types of Pyrenean river regimes based on previous indices to identify possible groups of hydrological years. Due to the large number of calculated indices and their probable correlation, we performed a Principal Component Analysis (PCA) to select the most suitable indices to describe river regimes, and omitted those that could be redundant. The principal components result from a linear combination of the original variables (Jolliffe, 2002). Then, we selected the main components using the Kaiser criterion (Kaiser, 1974), preserving those with eigenvalues of 1.00 or more. Next, the selected components were orthogonally rotated using the varimax criterion (Kaiser, 1958). This is a position change of the reference axis on the origin which redistributes the variance and allows approximation of the obtained components to the original variables to be

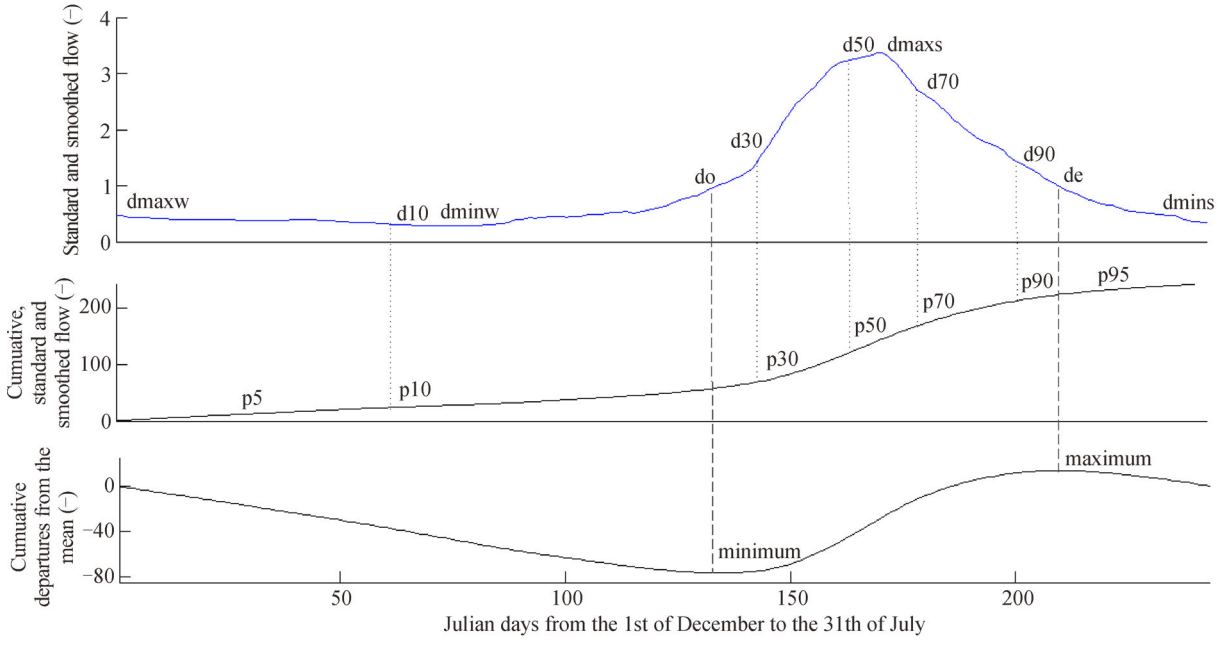

Fig. 2 Example of graphic calculation and placement of most of the hydrological indices in the standardized and smoothed 1988 annual hydrograph recorded in the gauging station of the Valira River, in La Seu D'Urgell. See Table 2.

Table 2 Indices used to describe the annual shape of the hydrograph between December and July

Index	Definition	References
maxs	Maximum value recorded during the snowmelt period or the spring/beginning of summer (March–July)	Adaptation of the indices day of spring maximum (DSM) from Morán-Tejeda et al. (2014) and Qmax from López-Moreno and García-Ruiz (2004)
dmaxs	Julian day when maxs occurs. See Fig. 2	Adaptation of the index Dqmax from López-Moreno and García-Ruiz (2004)
mins	Minimum value recorded during the snowmelt period or the spring/beginning of summer (March–July)	
dmins	Julian day when mins occurs. See Fig. 2	
maxw	Maximum value recorded during the period of low flows of winter (December–February)	
dmaxw	Julian day when maxw occurs. See Fig. 2	
minw	Minimum value recorded during the period of low flows of winter (December–February)	Adaptation of the index Qmin from López-Moreno and García-Ruiz (2004)
dminw	Julian day when minw occurs. See Fig. 2	Adaptation of the index Dqmin from López-Moreno and García-Ruiz (2004)
MAMJJ	Snowmelt period fractional flow (ratio of March–July streamflow to December–July streamflow)	Adaptation of snowmelt season fractional flow (AMJJ) from Stewart et al. (2005)
do	Onset of spring pulse of streamflow (day when most of the flows are higher than the mean), calculated by cumulative departures from mean flow (as the minimum value). See Fig. 2	Adaptation of the algorithm from Cayan et al. (2001)
de	End of the spring pulse of streamflow (day of the maximum value of the cumulative departures from the mean flow). See Fig. 2	
d10, d30, d50, d70, d90	d50 is the Julian day that has 50% of the December–July streamflow; the other used indices are based on the d50. See Fig. 2	d50: adaptation of the index winter/spring center of volume date (WSCV) from Burn (2008)
p5, p95	5th and 95th percentiles of the December–July streamflow. See Fig. 2	Adaptation of percentiles from Burn (2008)

maximized (Richman, 1986), while maintaining orthogonality. The selected indices for characterization of the river regimes were those which had the strongest correlation (>0.70) with the selected components: maxw, dminw, MAMJJ, d30, d50, p5, do, and de.

After the most representative indices were selected, we performed an agglomerative hierarchical clustering to classify the hydrological years based on the values for each index (December–July period). This enabled identification of possible groups and patterns of the indices. We used the Euclidean distance as an indicator of the similarity between years, and Ward's method (Ward, 1963) to combine the groups at several stages of the process to minimize intra-group variance and maximize between-group variance. According to Morán-Tejeda et al. (2012), the selection of the number of groups was based on the grouping coefficient (which indicates the Euclidean distance between combined groups at each stage) and Wilks's Lambda (which indicates the relationship between intra-group variance and total variance). We selected the ideal number of groups by inspection of graphs that show discontinuities in each value.

3.2.2 Assessment of the drivers of the nival signal

We assessed whether there were statistically significant differences between types of river regimes according to a basin's elevation and longitude and according to existing SWE in the basins (Ara, Aragón, Ésera, Segre, and Veral). None of the analyzed variables had normal distributions (Kolmogorov-Smirnov test, $p<0.05$), so we used non-parametric methods. The Kruskal-Wallis test was used to compare more than two samples (H statistic; Kruskal and Wallis, 1952) and the Mann-Whitney U test was used to compare two samples (Z statistic; Mann and Whitney, 1947, Appendix C).

Correlations between the streamflow series and other hydrological and climatic data series were estimated in the Ésera and Aragón basins by Pearson's R statistic. Linear trends were removed from these series prior to calculation of the correlations to avoid spurious significant R values that could occur when two series have similar monotonic trends (Wu et al., 2007).

3.2.3 Trend analysis

We searched for monotonic trends in the hydrological indices by use of the Mann-Kendall test (Mann, 1945; Kendall, 1975) (which calculates the statistical significance, magnitude, and sign of the trends) and Thiel-Sen's slope estimator (which estimates the slope of the linear trend). Both tests are robust against non-normal distribu-

tions and outliers, and are frequently used for trend detection in climatic and hydrological data (Burn and Hag Elnur, 2002; Yue et al., 2002; Chen and Grasby, 2009; Irannezhad et al., 2015; Sankey et al., 2015).

4 Results

4.1 Types of river regimes and their spatial and temporal distribution

The PCA yielded the following indices: maxw, dminw, MAMJJ, d30, d50, p5, do, and de based on a correlation greater than 0.70. With these indices, we identified 4 types of river regimes in the Spanish Pyrenean rivers (Fig. 3) based on the indices selected above and the clustering procedure. These types of river regimes were present in 8% (Type 1), 11% (Type 2), 56% (Type 3), and 25% (Type 4) of the total analyzed years, with only 5 outlier years excluded. The Type 1 regime had the least-defined nival character, because there was almost no difference between the maximum winter streamflow (maxw in Table 3) and the maximum spring flow (maxs = 1.81±0.51). In contrast, the Type 4 regime had the strongest nival signal, with a delay in the period of high river flows and an average onset on April 12 and end later than July 31. Regime Types 2 and 3 were intermediate between Types 1 and 4. There is indeed similarities between Type 3 and Type 4, the distinguishing feature between both is the delay in the period of high river flows in types 4 beside types 3: on average the onset of snow melt occurred 14 days later, the 30 and 50% of December–July streamflow is reached 10 and 13 days later respectively, and specially the end of snow melt occurred more than 38 days later. Table 3 shows that values of discharge associated with snowmelt increase from Type 1 to Type 4 and that do, d30 and d50 occur increasingly later from Type 1 to Type 4. The value of maxw also declines from Type 1 to Type 4. Regime Type 3 had the highest values of spring flow (maxs = 2.61±0.62).

A basin's longitude ($H = 21.06$, $p < 0.001$) and elevation

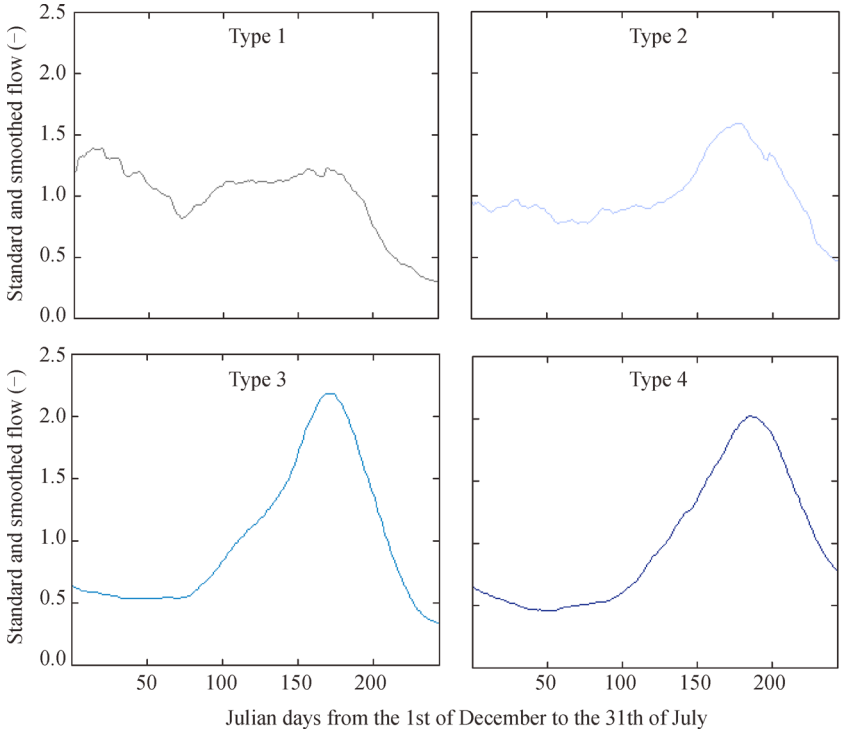

Fig. 3 Standardized and smoothed annual hydrographs of the four types of river regimes in the Spanish Pyrenees (Type 1, 2, 3, and 4). Only the hydrological year (December–July) was used for this analysis.

Table 3 Selected mean indices for each type of river regime

Type	maxw	dminw /days	MAMJJ /%	d30 /days	d50 /days	p5	do [a)] /days	de [b)] /days
1	1.88	56	58.23	60	110	0.28		
2	1.61	44	68.02	85	139	0.39	117	
3	0.93	49	79.23	116	151	0.31	119	205
4	0.88	48	81.11	126	164	0.32	133	

[a)] do index was not calculated for regime Type 1. [b)] de index was only calculated for regime Type 3.

($H = 86.04$, $p < 0.001$) partially explain the geographical segregation of river regimes (Fig. 4). Regime Type 3, the most common type in the study area (56%), was mostly present in the eastern basins (Segre 77±7%, Carol 81%, Valira 81%). Regime Types 1 and 2 were less common in the eastern region (Segre 6±2% and 4±7%, none in Carol) than in the western region (Veral 36% and 20%, Aragón 23% and 19%). Regime Type 4 mainly occurred in basins at the highest massifs, and was dominant in the Ésera River (73%), and to a lesser extent in the eastern basins; Type 4 was rare or absent in the westernmost basins.

Figure 5 shows the yearly evolution of river regimes in the studied basins. In rivers with longer records a trend toward less frequent regime types 3 and 4 and more frequent types 1 and 2 is observed from the 1980's decade onwards. e.g., in the Aragón River, Type 1 occurred 5 times between 1985 and 2010, and only twice between 1950 and 1980; and Type 4 occurred 5 times between 1950 and 1980 and only once between 1980 and 2010. Notably, some of the regime shifts occurred simultaneously in most of the analyzed stations (e.g., 1963, 1972, and 1997), with an increase of regimes that had weak nival signals.

Moreover, there was a shift toward an earlier spring pulse of streamflow from 1985 to 2010 (negative trends for do, de, d30, and d50, Appendix A) and a slight increase in the relative strength of the winter flows relative to the spring flows (negative trend for MAMJJ index and positive trend for maxw index). However, most of these results are not statistically significant according to the Mann-Kendall test.

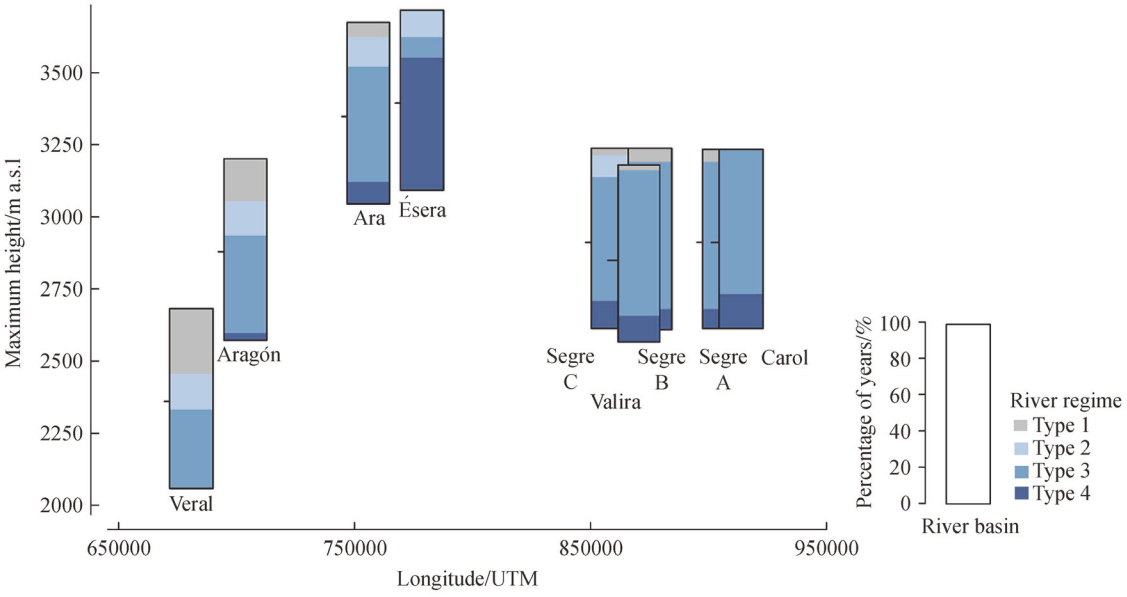

Fig. 4 Geographical distribution of the different types of river regimes according to basin maximum elevation and gauging station longitude (differences in latitude were negligible). The bars show the percentage of hydrological years (1985–2010) analyzed at each gauging station that had different types of river regimes.

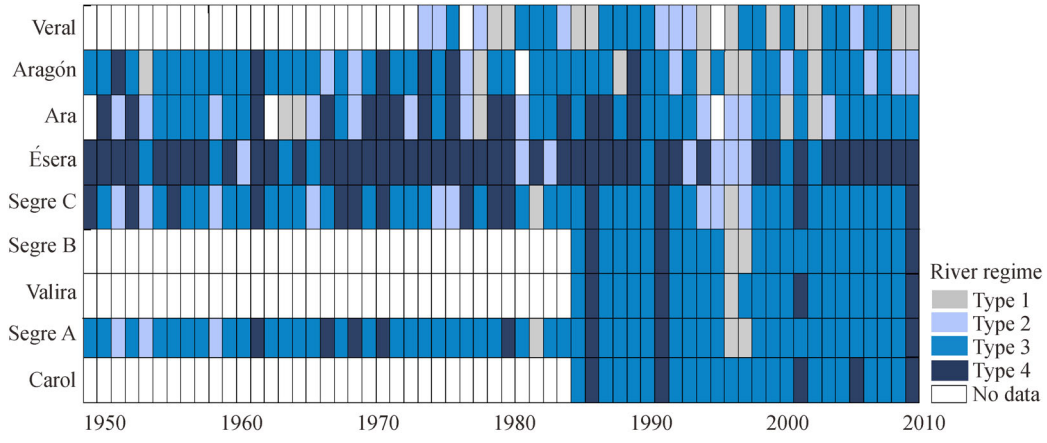

Fig. 5 Temporal variability of the different types of river regimes. Gauging stations were arranged from top to bottom by location (west to east).

4.2 Effect of snow on the nival signal

Figure 6 shows the distribution of standardized SWE across the hydrological years for each type of river regime in the studied basins from 1986 to 2010. Although the data has high dispersion (long "boxes" and "whiskers"), there were generally below-normal SWE values when regime Types 3 and 4 occurred, and above-normal SWE values when regimes 1 or 2 occurred, contrary to expectations. We only found statistically significant differences between groups of years when accounting for the SWE accumulated during January. Specifically, the SWE was significantly greater when regime Type 1 ($Z = 2.29$, $p < 0.05$) and Type 2 ($Z = 2.92$, $p < 0.01$) — rather than Type 3 — occurred in the Ara River. Similarly, the SWE was greater when the Ésera River had a Type 2 regime than a Type 4 regime ($Z = 3.14$, $p < 0.01$). We confirmed this somewhat surprising finding by examination of specific examples (Appendix B). This analysis confirmed a clear mismatch between yearly amount of accumulated snow and the strength of the nival character of the river regimes.

We graphically examined this unexpected behavior by plotting streamflows, snowmelt, and precipitation for years that had the most characteristic shapes of each type of hydrograph (Fig. 7). These results indicate that streamflow during years with apparently well-defined nival signals (Type 3 in Fig. 7(c), Type 4 in Fig. 7(d)) is due to an absence of precipitation during winter and a large amount of rainfall during spring; snowmelting had only a marginal effect. In other words, spring precipitation can produce increased streamflow during months when snowmelting typically occurs, and give rise to a false nival signal by comparing with identical types of nival signal non precipitation driven (Type 3 in Fig. 7(e), Type 4 in Fig. 7(f)). Furthermore, in years that had regimes normally associated with a low nival signal (Type 1 in Fig. 7(a), Type 2 in Fig. 7(b)), the amount and hydrological effect of snowmelt was actually greater than in years with Type 3 and Type 4 regimes, even though spring rainfalls also had a large effect in producing the false nival signal.

The above observation was surprising, but this pattern was clearly present in some specific years. However, our analysis of the long-term averages (1979–2005) of streamflows, precipitation, and snowmelt (Fig. 8) indicated that streamflow had a clearer seasonal response to snowmelt in the Ésera and Aragón basins. Our analysis showed that precipitation and snowmelt had high correlations with streamflow in both basins during spring. During

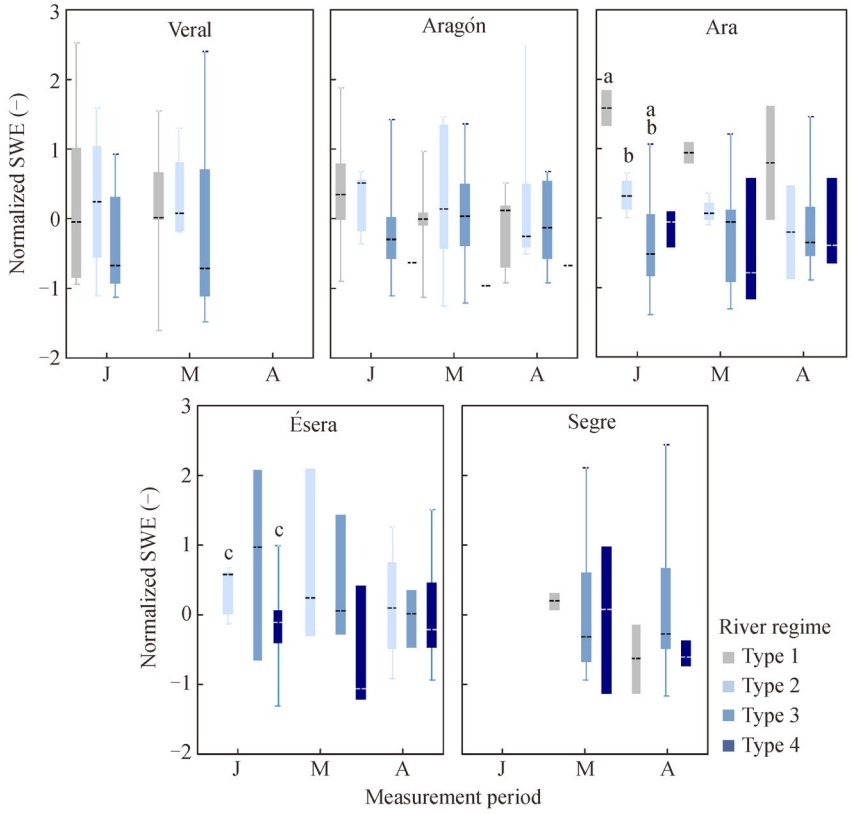

Fig. 6 SWE in the headwaters of the studied river basins with different types of river regimes from 1986 to 2010. Line: median; box: 25th and 75th percentiles; whiskers: 1st and 99th percentiles. The measurement periods are: J (January), M (March), and A (April). Identical letters indicate a statistically significant difference ($p < 0.05$) according to the Mann-Whitney test.

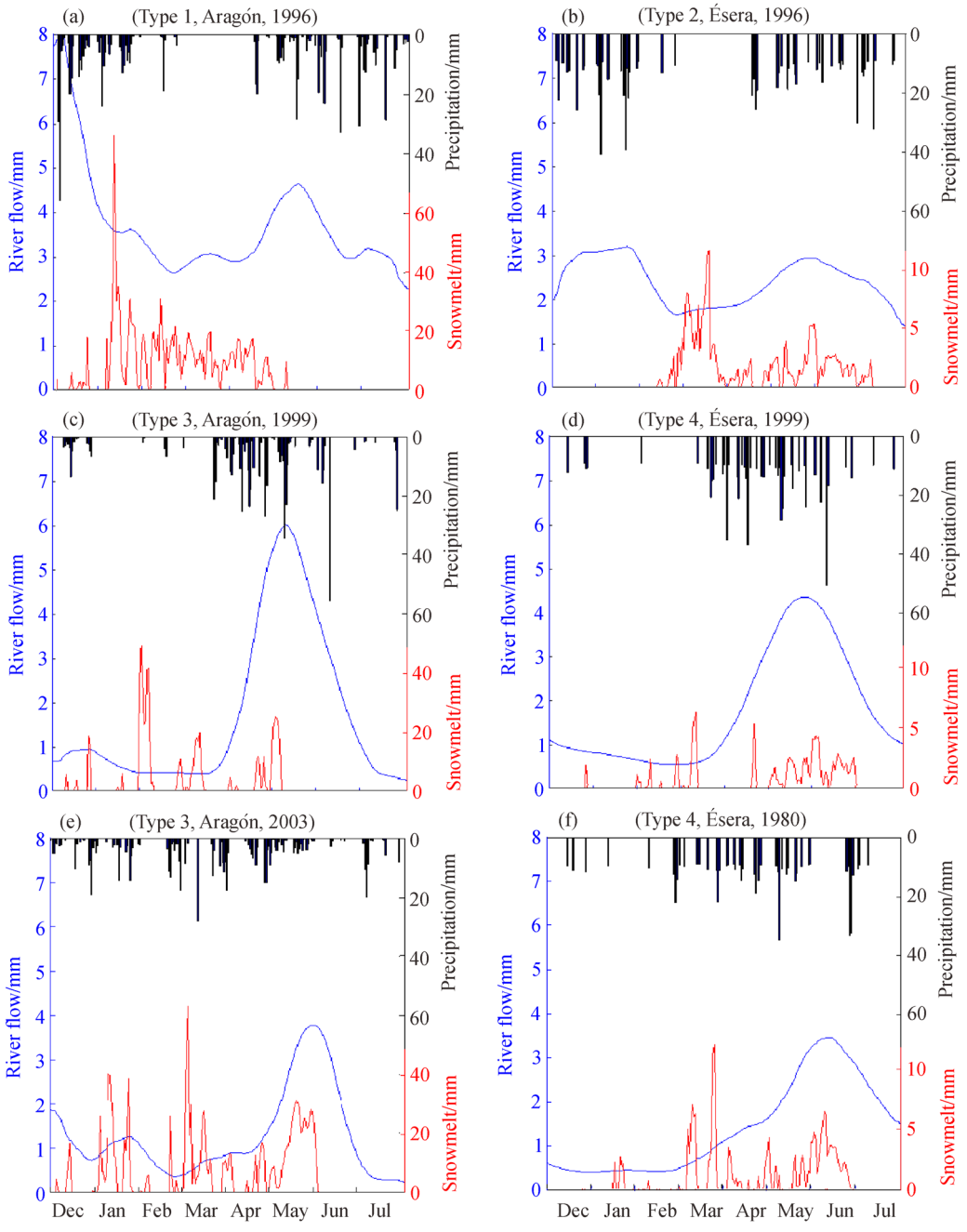

Fig. 7 Examples of short-term evolution of river flow, snowmelt, and precipitation in the Ésera and Aragón basins according to the type of river regime. Data are daily averages of each selected hydrologic year.

winter, the Ésera basin river flows had high correlations with precipitation, but low correlations with snowmelt. In the Aragón basin, precipitation had an even greater correlation with winter river flows, and snowmelt also correlated with flows. On the other hand, in both basins a higher minimum temperature was related to greater streamflow, mainly during the winter months, with the exception of the Aragón basin during spring. All correlations were statistically significant ($p < 0.05$), except for that between winter snowmelt and flow of the Ésera river. We found no significant correlations between the mean basin maximum temperature and river flow ($R < |0.15|$).

5 Discussion

This study showed that it is possible to distinguish four different types of river regimes on the southern side of the Pyrenees according to the strength of the nival signal. It

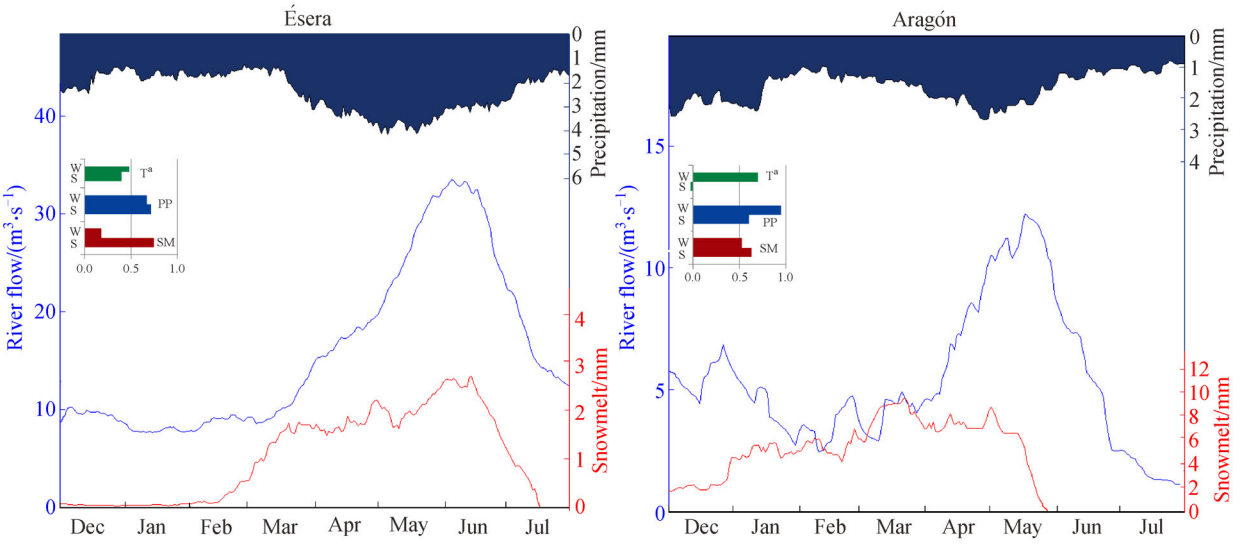

Fig. 8 Long-term evolution of river flow, snowmelt, and precipitation in the Ésera and Aragón basins. Data are daily medians of the complete data series (1979–2005). Correlations (Pearson's *R*) between the season (W: winter, S: spring) river flows, and the corresponding accumulated precipitation (PP), snowmelt (SM), and minimum temperature (T^a) are indicated.

also showed that the occurrence of different types of regimes is related to the elevation and longitude of the river basin, although different types of regimes occurred with varying frequencies in each basin throughout the study period. These findings, combined with data on snow accumulation, snowmelting, precipitation, and temperature in some of the studied basins, allowed us to assess the role of these variables on the strength of the nival signal. This analysis demonstrated that snow accumulation and snowmelt cannot entirely explain the interannual variability of these river regimes. In contrast to expectations, the seasonal distribution of precipitation plays a key role in determining the strength of the nival signal.

In general, snow markedly modulates the regimes of Pyrenean rivers. Thus flows during winter are low and uniform, and flows during spring are greater and have fluctuations (García-Ruiz et al., 1985; Beguería et al., 2003; López-Moreno and García-Ruiz, 2004). This pattern occurs throughout the hydrological year, although this study and previous studies have found some interannual anomalies. Bejarano et al. (2010) classified river regimes in the Ebro basin and classified the Pyrenean stations as nivo-pluvial regimes. Morán-Tejeda et al. (2014) used daily streamflow series to classify rivers in the Spanish Mountains as pluvial-nival, nival-pluvial, or pure snowmelt-dominated regimes; they classified Pyrenean rivers as pluvial-nival or as pure snowmelt-dominated regimes. In the present study, we identified 4 types of river regimes. Our Type 1 is similar to the pluvial-nival regime, and our Type 4 is similar to the snowmelt-dominated regime described by Morán-Tejeda et al. (2014). The spatial distribution of our different types of river regimes (Fig. 4) is consistent with the responses of river regimes of the Central Pyrenees described by López-Moreno and García-Ruiz (2004), with reduced Oceanic influence in the eastern region and an effect of basin elevation. In particular, we observed fewer Type 1 and Type 2 regimes in the eastern region (Fig. 4); the western basins had no low flows during winter or had lower flows than basins in the eastern region. This supports the observation that basins influenced by the Atlantic Ocean, such as the Veral River Basin, have abundant winter rainfalls but their relatively low elevations do not allow large snow accumulation (García-Ruiz et al., 1985). In contrast, we observed a higher frequency of river regime Type 4 in basins at the highest massifs (Fig. 4), in the Central Pyrenees, where large snow accumulation is possible. In these basins, there is a delay in the onset of snow melting (mid-April on average) and high spring flows, and on average more than 80% of the total flow occurs between March and July. The clearest example of this pattern is the Ésera River Basin, where the end of the spring pulse can extend beyond July 31. Further east, due to the influence of the Mediterranean and continental climate, there is reduced winter precipitation, and therefore reduced snow input (García-Ruiz et al., 1985). This means that the most common river regime in this area is Type 3, in which there is an earlier and slightly smaller spring pulse (Fig. 4).

In addition to the spatial variability in river regimes, there was also a temporal variability. From the 1980s, we observed a general reduction of Type 4 and an increase of Types 1 and 2 (Fig. 5), although these changes were not statistically significant. Even in the longer data series (1950–2010), regime changes occurred simultaneously in most of the analyzed stations. Overall, peak flows became less important during more recent decades, whereas winter

flows increased. These observations are consistent with previous findings in the Pyrenees and other mountain ranges of the Iberian Peninsula (López-Moreno and García-Ruiz, 2004; Morán-Tejeda et al., 2014), the Alps (Bard et al., 2010; Kormann et al., 2015), North America (Cayan et al., 2001; Stewart et al., 2005; Moore et al., 2007; Burn, 2008; Clow, 2010), and Japan (Yamanaka et al., 2012).

For mountain rivers, knowledge of snowpack conditions and related processes is required to explain the seasonality of low and high flows (López-Moreno and García-Ruiz, 2004; Whitaker et al., 2008; Yang et al., 2009; Godsey et al., 2014; Kormos et al., 2014). In fact, the association of certain types of river regimes with certain rivers in this study indicates that stored snow can have different effects in different river basins in the Pyrenees. In the Central Pyrenees, previous studies considered snowmelt as the main source of spring discharges (García-Ruiz et al., 1985; López-Moreno and García-Ruiz, 2004). But, we found that the amount of accumulated snow and snowmelt do not always determine the strength of the nival signal; in fact, some years with apparently well-defined nival signals had less SWE in the headwaters and later snowmelt than years with weaker nival signals. Therefore, snow cannot be considered the sole factor in explaining the interannual variability of Pyrenean river regimes. As we expected, high winter flows, characteristic of rivers with weak nival signals, were greatly influenced by rain. But surprisingly, most years with strong nival signals (low winter flows and high spring flows), had a spring pulse that was greatly induced by rain (Figs. 7(c) and 7(d)). The precipitation role in the hydrograph signal was detected also in the long-term analysis (Fig. 8). Indeed, we found that precipitation and snowmelt correlated with spring streamflow.

We have shown that large rainfall events affect streamflow as well, and these may lead to greatest spring peakflows. Therefore, spring rainfalls will introduce an extra source of water that will sum up to the water from snowmelt, contributing to the spring peakflows characteristic of mountain rivers. If the rain events fall onto the snow cover (rain-on-snow event), the snowmelt will accelerate, enhancing the peak-shape of the hydrograph (Singh et al., 1997; Pradhanang et al., 2013). Thus, some river regimes had nival patterns of discharge during years when there was low snow accumulation during winter, but high precipitation in spring. Similarly, Lana-Renault et al. (2011) studied a Central Pyrenean basin and also fund some peakflows were accompanied by rainfall events. In particular, they reported an increase in discharge at the beginning of the snowmelt period due to large rainfalls that occurred through the end of March and the beginning of April. Likewise, Morán-Tejeda et al. (2014) showed that large amounts of precipitation matched the spring pulses in pure snowmelt-dominated river regimes in the Spanish mountain ranges, and the magnitude of the rainfalls were even larger than those that occurred in rivers with nival-pluvial regimes. Also, pluvial-nival regimes had the greatest amount of precipitation during spring, even higher than that during winter. Ryberg et al. (2016) studied streams dominated by snowmelt in the north-central USA and reported that most of them experienced a spring peak caused by snow accumulation throughout the winter and its subsequent melting, but in other cases spring rains caused the peaks. Similarly, this study discerns the peaks that occur in the spring from snowmelt, rain on snow, or spring rain. On the other hand, we found that warmer winters were associated with higher winter flows, but there was no significant correlation between temperature and accumulated streamflow during spring (Fig. 8). During warm winters, there is less snow accumulation: as the temperature often exceeds 0°C, the amount of snowfall declines as rainfall increases, leading to increased river flows at that time. A warm spring leads to a reduced duration of snowpack because of an earlier onset of melting, but does not necessarily impact the magnitude of the spring flows (Cayan, 1996; Stewart et al., 2005; Stewart, 2009; Clow, 2010; Morán-Tejeda et al., 2014).

The results of this study should be considered when indices derived from hydrographs are used as indicators of climate change or snow evolution in other catchments and mountain regions (López-Moreno and García-Ruiz, 2004; Whitaker et al., 2008; Yang et al., 2009). We confirmed that when river flow values are averaged over several years, the pattern of low winter flows and high spring flows occur when more snow accumulates in the headwaters. However, when individual years are considered, the interaction between snow melting, liquid precipitation, and temperature may deviate from this pattern, and this could lead to incorrect conclusions when trend analyses are conducted. Special attention must be given to regions with a strong seasonal pattern of precipitation, such the Mediterranean. In these regions, spring rainfall is a major or even the largest source of precipitation (De Luis et al., 2010; Tuset et al., 2016). As a consequence, a greater spring rainfall, due to increased influence from the Mediterranean (Camarasa-Belmonte and Soriano, 2014) or interannual variability (Gaetani et al., 2011), can mask the effect of snowmelting on river flows.

6 Conclusions

The main conclusions of this work can be summarized as follows:

1) There were four main types of river regimes during the snow accumulation and melting periods in the Spanish Pyrenees, with Type 1 having the weakest nival signal and Type 4 having the strongest.

2) Longitude and elevation-mediated climatic gradients along the Pyrenees are major factors in determining the type of river regime in the study area.

3) The inter-annual variability in SWE in the analyzed

basins do not by themselves account for type of river regime. Instead, rainfall and temperature are key factors explaining winter and spring flow modulation during many of the studied years. This suggests that, at least in short-term analysis, the role of snow on streamflow variability can overwhelmed by liquid precipitation.

Acknowledgements This study was funded by the research project CGL2014-52599-P, "Estudio del manto de nieve en la montaña española y su respuesta a la variabilidad y cambio climatico" from the Spanish Ministry of Economy and Competitiveness. The authors thank the ERHIN program for providing the snow data used in this study.

References

Adam J C, Hamlet A F, Lettenmaier D P (2009). Implications of global climate change for snowmelt hydrology in the twenty-first century. Hydrol Processes, 23(7): 962–972

Auble G T, Friedman J M, Scott M L (1994). Relating riparian vegetation to present and future streamflows. Ecol Appl, 4(3): 544–554

Bard A, Renard B, Lang M (2010). Observed trends in the hydrologic regime of Alpine catchments. In: EGU General Assembly Conference Abstracts, vol. 12, p. 11627

Barnett T P, Adam J C, Lettenmaier D P (2005). Potential impacts of a warming climate on water availability in snow-dominated regions. Nature, 438(7066): 303–309

Beguería S, López-Moreno J I, Lorente A, Seeger M, García-Ruiz J M (2003). Assessing the effect of climate oscillations and land-use changes on streamflow in the Central Spanish Pyrenees. Ambio, 32 (4): 283–286

Bejarano M D, Marchamalo M, de Jalón D G, del Tánago M G (2010). Flow regime patterns and their controlling factors in the Ebro basin (Spain). J Hydrol (Amst), 385(1): 323–335

Beniston M (2012). Is snow in the Alps receding or disappearing? Wiley Interdiscip Rev Clim Chang, 3(4): 349–358

Burn D H (2008). Climatic influences on streamflow timing in the headwaters of the Mackenzie River Basin. J Hydrol (Amst), 352(1-2): 225–238

Burn D H, Hag Elnur M A H (2002). Detection of hydrologic trends and variability. J Hydrol (Amst), 255(1): 107–122

Camarasa-Belmonte A M, Soriano J (2014). Empirical study of extreme rainfall intensity in a semi-arid environment at different time scale. J Arid Environ, 100–101: 63–71

Cayan D R (1996). Interannual climate variability and snowpack in the western United States. J Clim, 9(5): 928–948

Cayan D R, Dettinger M D, Kammerdiener S A, Caprio J M, Peterson D H (2001). Changes in the onset of spring in the Western United States. Bull Am Meteorol Soc, 82(3): 399–415

Chauvin G M, Flerchinger G N, Link T E, Marks D, Winstral A H, Seyfried M S (2011). Long-term water balance and conceptual model of a semi-arid mountainous catchment. Journal of Hydrolology, 400 (1–2): 133–143

Chen Z, Grasby S E (2009). Impact of decadal and century-scale oscillations on hydroclimate trend analyses. Journal of Hydrolology, 365(1–2): 122–133

Clow D W (2010). Changes in the timing of snowmelt and streamflow in Colorado: a response to recent warming. J Clim, 23(9): 2293–2306

De Luis M, Brunetti M, Gonzalez-Hidalgo J C, Longares L A, Martin-Vide J (2010). Changes in seasonal precipitation in the Iberian Peninsula during 1946–2005. Global Planet Change, 74(1): 27–33

Dedieu J P, Lessard-Fontaine A, Ravazzani G, Cremonese E, Shalpykova G, Beniston M (2014). Shifting mountain snow patterns in a changing climate from remote sensing retrieval. Sci Total Environ, 493: 1267–1279

Del Barrio G, Creus J, Puigdefábregas J (1990). Thermal seasonality of the high mountains belt of the Pyrenees. Mt Res Dev, 10(3): 227–233

Foy C, Arabi M, Yen H, Gironás J, Bailey R T (2015). Multisite assessment of hydrologic processes in snow-dominated mountainous river basins in Colorado using a watershed model. J Hydrol Eng, 20 (10): 04015017

Gaetani M, Baldi M, Dalu G A, Maracchi G (2011). Jetstream and rainfall distribution in the Mediterranean region. Nat Hazards Earth Syst Sci, 11(9): 2469–2481

García-Ruiz J M, López-Moreno J I, Vicente-Serrano S M, Lasanta–Martínez T, Beguería S (2011). Mediterranean water resources in a global change scenario. Earth Sci Rev, 105(3-4): 121–139

García-Ruiz J M, Puigdefábregas T J, Creus-Novau J (1985). Los recursos hídricos superficiales del Alto Aragón. Huesca: Instituto de Estudios Altoaragoneses

Godsey S E, Kirchner J W, Tague C L (2014). Effects of changes in winter snowpacks on summer low flows: case studies in the sierra nevada, California, USA. Hydrol Processes, 28(19): 5048–5064

Herrera S, Gutiérrez J M, Ancell R, Pons M R, Frías M D, Fernández J (2012). Development and analysis of a 50‐year high‐resolution daily gridded precipitation dataset over Spain (Spain02). Int J Climatol, 32(1): 74–85

Hinch S G, Healey M C, Diewert R E, Henderson M A, Thomson K A, Hourston R, Juanes F (1995). Potential effects of climate change on marine growth and survival of Fraser River sockeye salmon. Can J Fish Aquat Sci, 52(12): 2651–2659

Irannezhad M, Ronkanen A K, Kløve B (2015). Effects of climate variability and change on snowpack hydrological processes in Finland. Cold Reg Sci Technol, 118: 14–29

Jolliffe I (2002). Principal Component Analysis and Factor Analysis. Principal Component Analysis. Springer Series in Statistics, 150–166

Kaiser H F (1958). The varimax criterion for analytic rotation in factor analysis. Psychometrika, 23(3): 187–200

Kaiser H F (1974). An index of factorial simplicity. Psychometrika, 39 (1): 31–36

Kendall M (1975). Multivariate Analysis. London: Charles Griffin

Kormann C, Francke T, Bronstert A (2015). Detection of regional climate change effects on alpine hydrology by daily resolution trend analysis in Tyrol, Austria. Journal of Water and Climate Change, 6 (1): 124–143

Kormos P R, Marks D, McNamara J P, Marshall H P, Winstral A, Flores A N (2014). Snow distribution, melt and surface water inputs to the soil in the mountain rain-snow transition zone. Journal of Hydrology, 519(PA): 190–204,

Kruskal W H, Wallis W A (1952). Use of ranks in one-criterion variance analysis. J Am Stat Assoc, 47(260): 583–621

Lana-Renault N, Alvera B, García-Ruiz J M (2011). Runoff and sediment transport during the snowmelt period in a Mediterranean high-mountain catchment, . Arct Antarct Alp Res, 43(2): 213–222

López R, Justribó C (2010). The hydrological significance of mountains: a regional case study, the Ebro River basin, northeast Iberian Peninsula. Hydrol Sci J, 55(2): 223–233

López-Moreno J I (2005). Recent variations of snowpack depth in the Central Spanish Pyrenees. Arct Antarct Alp Res, 37(2): 253–260

López-Moreno J I, Beniston M, García-Ruiz J M (2008). Environmental change and water management in the Pyrenees: facts and future perspectives for Mediterranean mountains. Global Planet Change, 61 (3): 300–312

López-Moreno J I, Fassnacht S R, Beguería S, Latron J (2011b). Variability of snow depth at the plot scale: implications for mean depth estimation and sampling strategies. Cryosphere, 5(3): 617–629

López-Moreno J I, Fassnacht S R, Heath J T, Musselman K N, Revuelto J, Latron J, Morán-Tejeda E, Jonas T (2013). Small scale spatial variability of snow density and depth over complex alpine terrain: implications for estimating snow water equivalent. Adv Water Resour, 55: 40–52

López-Moreno J I, García-Ruiz J M (2004). Influence of snow accumulation and snowmelt on streamflow in the central Spanish Pyrenees. Hydrol Sci J, 49(5) doi: 10.1623/hysj.49.5.787.55135

López-Moreno J I, Goyette S, Beniston M (2009). Impact of climate change on snowpack in the Pyrenees: horizontal spatial variability and vertical gradients. J Hydrol (Amst), 374(3): 384–396

López-Moreno J I, Vicente-Serrano S M, Morán-Tejeda E, Zabalza J, Lorenzo-Lacruz J, García-Ruiz J M (2011a). Impact of climate evolution and land use changes on water yield in the Ebro basin. Hydrol Earth Syst Sci, 15(1): 311–322

López-Moreno J I, Revuelto J, Rico I, Chueca-Cía J, Julián A, Serreta A, Serrano E, Vicente-Serrano S M, Azorín-Molina C, Alonso-González E, García-Ruiz J M (2016). Thinning of the Monte Perdido Glacier in the Spanish Pyrenees since 1981. Cryosphere, 10(2): 681–694

López-Moreno J I, Vicente-Serrano S M, Zabalza J, Revuelto J, Gilaberte M, Azorín-Molina C, Morán-Tejeda E, García-Ruiz J M, Tague C (2014). Respuesta hidrológica del Pirineo central al cambio ambiental proyectado para el siglo XXI. Pirineos, 169(0): e004

Lute A C, Abatzoglou J T, Hegewisch K C (2015). Projected changes in snowfall extremes and interannual variability of snowfall in the western United States. Water Resour Res, 51(2): 960–972

Mann H B (1945). Nonparametric tests against trend. Econometrica, 13 (3): 245–259

Mann H B, Whitney D R (1947). On a test of whether one of two random variables is stochastically larger than the other. Ann Math Stat, 18(1): 50–60

Marti R, Gascoin S, Houet T, Ribière O, Laffly D, Condom T, Monnier S, Schmutz M, Camerlynck C, Tihay J P, Soubeyroux J M, René P (2015). Evolution of Ossoue Glacier (French Pyrenees) since the end of the Little Ice Age. Cryosphere, 9(5): 1773–1795

Masiokas M H, Villalba R, Luckman B H, Mauget S (2010). Intra- to multidecadal variations of snowpack and streamflow records in the Andes of Chile and Argentina between 30° and 37°S. J Hydrometeorol, 11(3): 822–831

Moore J N, Harper J T, Greenwood M C (2007). Significance of trends toward earlier snowmelt runoff, Columbia and Missouri Basin headwaters, western United States. Geophys Res Lett, 34(16) doi: 10.1029/2007GL031022

Morán-Tejeda E, Herrera S, López-Moreno J I, Revuelto J, Lehmann A, Beniston M (2013). Evolution and frequency (1970-2007) of combined temperature-precipitation modes in the Spanish mountains and sensitivity of snow cover. Reg Environ Change, 13(4): 873–885

Morán-Tejeda E, Lorenzo-Lacruz J, López-Moreno J I, Ceballos-Barbancho A, Zabalza J, Vicente-Serrano S M (2012). Reservoir Management in the Duero Basin (Spain): impact on River Regimes and the Response to Environmental Change. Water Resour Manage, 26(8): 2125–2146

Morán-Tejeda E, Lorenzo-Lacruz J, López-Moreno J I, Rahman K, Beniston M (2014). Streamflow timing of mountain rivers in Spain: recent changes and future projections. J Hydrol (Amst), 517: 1114–1127

Morán-Tejeda E, Zabalza J, Rahman K, Gago-Silva A, López-Moreno J I, Vicente-Serrano S, Lehmann A, Tague C L, Beniston M (2015). Hydrological impacts of climate and land-use changes in a mountain watershed: uncertainty estimation based on model comparison. Ecohydrology, 8(8): 1396–1416

Peña J, Lozano M (2004). Las unidades del relieve aragonés, Geografía Física de Aragón, Aspectos Generales Y Temáticos. Zaragoza: Universidad de Zaragoza

Poff N, Brinson M M, Day J (2002). Aquatic ecosystems and global climate change.Arlington: Pew Center on Global Climate Change

Pradhanang S M, Frei A, Zion M, Schneiderman E M, Steenhuis T S, Pierson D (2013). Rain-on-snow runoff events in New York. Hydrol Processes, 27(21): 3035–3049

Revuelto-Benedí J, López-Moreno J I, Morán-Tejada E, Fassnacht S R, Vicente-Serrano S M (2012). Variabilidad interanual del manto de nieve en el Pirineo: tendencias observadas y su relación con índices de teleconexión durante el periodo 1985-2011. In: 8° Congreso Internacional sobre Cambio climático, Extremos e Impactos. Salamanca: Asociación Española de Climatología, 613–621

Richman M B (1986). Rotation of principal components. J Climatol, 6 (3): 293–335

Ryberg K R, Akyüz F A, Wiche G J, Lin W (2016). Changes in seasonality and timing of peak streamflow in snow and semi-arid climates of the north-central United States, 1910–2012. Hydrol Processes, 30(8): 1208–1218

Sankey T, Donald J, McVay J, Ashley M, O'Donnell F, Lopez S M, Springer A (2015). Multi-scale analysis of snow dynamics at the southern margin of the North American continental snow distribution. Remote Sens Environ, 169: 307–319

Schnorbus M, Werner A, Bennett K (2014). Impacts of climate change in three hydrologic regimes in British Columbia, Canada. Hydrol Processes, 28(3): 1170–1189

Singh P, Spitzbart G, Hübl H, Weinmeister H W (1997). Hydrological response of snowpack under rain-on-snow events: a field study. J Hydrol (Amst), 202(1): 1–20

Stewart I T (2009). Changes in snowpack and snowmelt runoff for key mountain regions. Hydrol Processes, 23(1): 78–94

Stewart I T, Cayan D R, Dettinger M D (2005). Changes toward Earlier Streamflow Timing across Western North America. J Climatol, 18(8): 1136–1155

Tuset J, Vericat D, Batalla R J (2016). Rainfall, runoff and sediment

transport in a Mediterranean mountainous catchment. Sci Total Environ, 540: 114–132

Viviroli D, Dürr H H, Messerli B, Meybeck M, Weingartner R (2007). Mountains of the world, water towers for humanity: typology, mapping, and global significance. Water Resour Res, 43(7): doi: 10.1029/2006WR005653

Ward J H Jr (1963). Hierarchical Grouping to Optimize an Objective Function. J Am Stat Assoc, 58(301): 236–244

Whitaker A C, Sugiyama H, Hayakawa K (2008). Effect of snow cover conditions on the hydrologic regime: case study in a pluvial-nival watershed, Japan. J Am Water Resour Assoc, 44(4): 814–828

Wu Z, Huang N E, Long S R, Peng C K (2007). On the trend, detrending, and variability of nonlinear and nonstationary time series. Proc Natl Acad Sci USA, 104(38): 14889–14894

Yamanaka T, Wakiyama Y, Suzuki K (2012). Is snowmelt runoff timing in the Japanese Alps region shifting toward earlier in the year? Hydrological Research Letters, 6(0): 87–91

Yang D, Zhao Y, Armstrong R, Robinson D (2009). Yukon River streamflow response to seasonal snow cover changes. Hydrol Processes, 23(1): 109–121

Yue S, Pilon P, Cavadias G (2002). Power of the Mann–Kendall and Spearman's rho tests for detecting monotonic trends in hydrological series. J Hydrol (Amst), 259(1): 254–271

Appendices

Appendix A

Change over time (decade $^{-1}$) in the Thiel-Sen's slope estimator for selected gauging stations. Gauging stations are arranged from top to bottom by location (west to east)

	Series	maxw	dminw /days	MAMJJ /%	d30 /days	d50 /days	p5	do [b] /days	de [c] /days
Veral	1975 – 2010	0.16	5.00	–0.60	–1.25	–3.75	**– 0.06**		
Aragón	1950 – 2010	0.06	3.28	**– 1.51**	–3.58	–2.20	0.00	2.19	
Ara	1951 – 2010	–0.01	–0.59	–0.10	0.00	–0.67	0.00	1.11	
Ésera	1950 – 2010	0.00	0.00	–0.73	–1.47	–1.85	**0.03**	1.26	
Segre C	1950 – 2010	0.05	–7.07	–1.16	–1.92	**– 3.45**	0.01	0.00	
Segre A	1950 – 2010	–0.03	0.00	0.49	1.43	–0.44	–0.01	1.34	–1.43
Veral	1985 – 2010	0.03	5.35	–0.97	–1.21	–2.50	–0.05		
Aragón	1985 – 2010	0.20	10.00	–3.91	–14.00	–4.71	0.00	0.00	
Ara	1985 – 2010	0.11	0.56	–1.37	–5.43	–5.00	0.02	–5.12	
Ésera	1985 – 2010	0.05	–4.00	–0.77	–4.44	–4.71	0.00	–3.33	
Segre C	1985 – 2010	0.31	–8.50	–1.98	–9.56	–8.06	0.01	–1.00	
Segre B	1985 – 2010	–0.09	–4.62	1.19	3.81	–1.67	–0.02	–2.73	–3.60
Valira	1985 – 2010	–0.03	0.48	2.89	4.62	0.00	**– 0.08**	–5.56	–1.55
Segre A	1985 – 2010	–0.11	2.35	2.36	5.63	0.00	–0.05	–5.00	–1.46
Carol	1985 – 2010	–0.04	9.09	1.72	0.91	–2.73	–0.03	**– 8.64**	–1.00
Mean	1985 – 2010	0.05	1.19	–0.09	–2.19	–3.26	–0.02	–3.92	–1.90
SD	1985 – 2010	0.14	6.27	2.26	6.74	2.62	0.03	2.76	1.15

Bold font: Statistically significant trend ($p < 0.05$) according to the Mann-Kendall test.
[b] do index trend was not calculated for rivers with more than 25% river regime Type 1.
[c] de index trend was only calculated for rivers with more than 75% river regime Type 3.

Appendix B

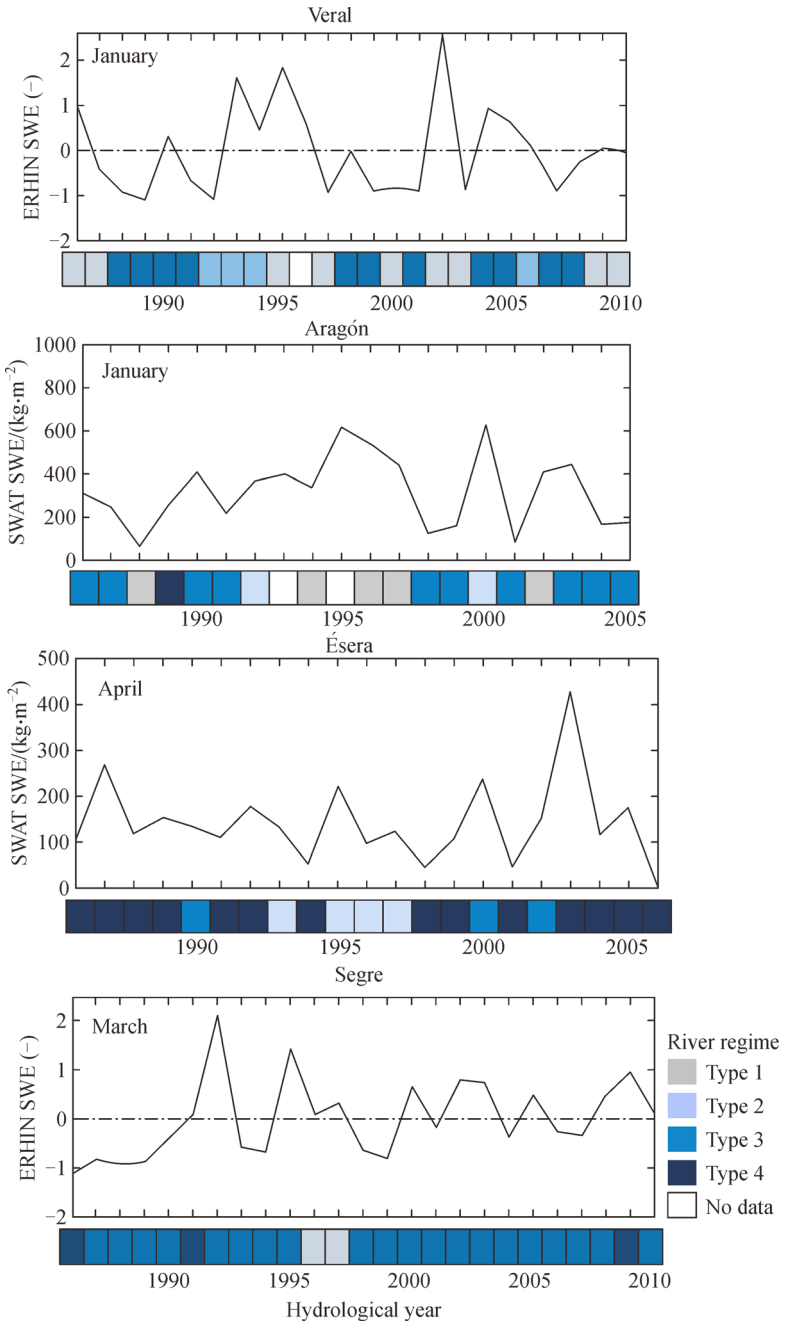

Examples of the inter-annual change in river regime and SWE in the analyzed river basins. SWE data source: ERHIN Programme or the SWAT model; measurement period: J (January), M (March), and A (April).

Appendix C

Calculation of Mann-Whitney *U* test
Adapted from Mann and Whitney (1947) for larger samples without ties.

$$U_1 = n_1 n_2 + \frac{n_1(n_1+1)}{2} - R_1,$$

$$U_2 = n_1 n_2 + \frac{n_2(n_2+1)}{2} - R_2,$$

where U is the statistic, n_1 is the size of sample 1, n_2 is the size of sample 2, R_1 is the rank sum for sample 1 and R_2 is the rank sum of sample 2. To calculate the rank sum of a sample, first assign numeric ranks to all the observations beginning with 1 for the smallest value, then add up the ranks. The value of U is the minimum U, it doesn't matter which sample is bigger. The distribution of U approximates a normal distribution in larger samples. In that case, the standardized value is Z:

$$Z = \frac{U\mu}{\sigma},$$

where the mean of U is $\mu = \frac{n_1 n_2}{2}$.

And the standard deviation of U is

$$\sigma = \sqrt{\frac{(n_1 n_2)(n_1 + n_2 + 1)}{12}}.$$

The significance of Z can be checked in tables of the normal distribution.

Calculation of Kruskal-Wallis test
Adapted from Kruskal and Wallis (1952) for samples without ties.

$$H = \left(\frac{12}{N(N+1)}\sum_{i=1}^{C}\frac{R_i^2}{n_i}\right) - 3(N+1),$$

where H is the statistic, C is the number of samples, N is the number of total cases, n is the number of cases in each sample, and R is the rank sum of each sample. The distribution of H approximates a Chi^2 distribution with k–1 degrees of freedom, thus the significance of H can be checked its tables of distribution:

$$H \geqslant x^2, c-1.$$